

CHARACTERIZATION OF ENHANCED HEAT TRANSFER SURFACES FOR DROP SPRAY COOLING SYSTEMS

Rachel C. Ahaiwe

August 16, 2024

Affiliation: Institut Jean Lamour
Address: Campus Artem 2 all André Guinier, 54000 Nancy
Email: rachelahaiwe@gmail.com

Key Words: Heatflux, Contact Angle, Wetting, Absorption, Surface Properties, Porosity

Abstract

Spray cooling serves diverse purposes. Surface temperature changes with significant heat flux variations. PEO-coated alumina and pure Aluminium polished and non-polished samples were characterized to determine their heat transfer properties for drop spray cooling systems. Scanning electron microscopy was used to investigate the surface morphology. Contact angle measurements were performed and the spreading dynamics of droplets at high temperatures were observed. The droplet lifetime was given as a function of various temperatures and the Weber number effect on lifetime was studied. The effect of surface characteristics on the heat transfer properties of a surface was extrapolated from the results of the study. The results indicate that PEO-coated samples can be utilized in low heat-flux applications requiring slow, sustained and gradual cooling as they have longer lifetimes, while the pure aluminium samples can be utilized for high heat-flux applications requiring rapid cooling.

1 Introduction

The exponential rise in technology has led to the miniaturization of electronic devices, high-energy laser systems, aerospace and defence systems and biomedical systems, which has subsequently led to a significant increase in power consumption and a high generation of heat on surface areas. It was shown that a 10°C rise in operation temperature would lead to a reduction in the lifetime of some electronic devices by 50%[1]. Hence, the need for effective thermal management and greater requirements in heat dissipation technology to ensure and improve the durability of devices via effective cooling. Additionally, the selection of thermal management techniques impacts device-level requirements and influences system-level design parameters, including weight and size[2].

Accumulated heat contributes to elevated operating temperatures, negatively affecting the lifetime and stability of equipment. Consequently, heat dissipation emerges as a bottleneck in the development of high-heat flux equipment[3]. Despite concerted efforts to minimize heat generation in integrated cir-

cuits, the persistent pursuit of faster clock speeds and increased packaging density in microprocessors necessitate more effective thermal management solutions than conventional air-cooling techniques to ensure the reliable operation of electronics[4]. The heat generated by modern electronic devices surpasses the capabilities of single-phase (air and liquid) cooling technologies, creating an urgent need for innovative cooling techniques to maintain electronic devices safely below their temperature damage limit[5]. Consequently, advancements in cooling systems must align with the rising heat removal demands. This progression starts with forced air convection, which is improved by compact finned heat sinks, moves to liquid-cooled microchannel arrays, and ultimately involves phase change heat transfer through boiling phenomena or from atomized sprays and jets. The selection of a suitable cooling technique depends on the specific application and critical system factors that must be met, including the maximum allowable heat flux, total heat load, precise temperature tolerances, reliability considerations, and overall power consumption. Additionally, the operating environment plays

a significant role, highlighting aspects like space utilization, system component complexity, technology maturity, and cost[6] In the past two decades, thorough research has been carried out on liquid cooling for the thermal management of high-heat-flux electronics. Unlike single-phase cooling, where surface temperature linearly correlates with heat flux, phase-change heat transfer allows for small temperature changes with significant heat flux variations due to the latent heat of vaporization[4]. Advanced cooling techniques utilizing two-phase heat transfer mechanisms leverage both exchanged heat and latent heat, consistently attracting attention for their inherent advantages. Spray cooling stands out as one of the most effective heat transfer techniques, capable of handling high heat flux and temperatures. It is widely recognized for achieving an optimal balance between high heat flux removal, uniform cooling over large areas, and the use of a diverse selection of liquids, making it one of the most promising technologies available.[2, 3, 7].

Currently, researchers actively explore the application of spray cooling in various domains, including electronics, aerospace, medicine, and battery thermal management, with practical implications in production and daily life. In medical and biomedical applications, spray cooling serves diverse purposes. It is widely employed to protect the skin from heat damage during laser treatments. Specifically, in the biomedical industry, cryogenic spray cooling is utilized to selectively precool human skin, particularly during laser treatments for port wine stain birthmarks and hair removal[8].

The thermal dissipation process in spray cooling encompasses the evaporation of the liquid film, augmented perturbation of the liquid film due to droplet impact, convective heat transfer, and evaporation. Extensive theoretical research has been conducted by scholars to unravel the mechanism and processes involved in spray cooling. Under constant pressure and when the hot surface temperature is below the boiling point of the cooling medium, spray cooling operates in a non-boiling regime(Fig.1). In this regime, forced convection and the evaporation of a thin liquid film stand out as the dominant heat transfer modes. Experimental results further validate that the heat transfer coefficient in the nucleate boiling regime exceeds that in saturated pool boiling. This improvement stems from spray cooling’s ability to enhance heat dissipation efficiency through forced convection and, more significantly, through phase transitions, including nuclear boiling on heated surfaces and nuclear boiling induced by secondary nucleation[9]. It was shown that the dynamic Leidenfrost tempera-

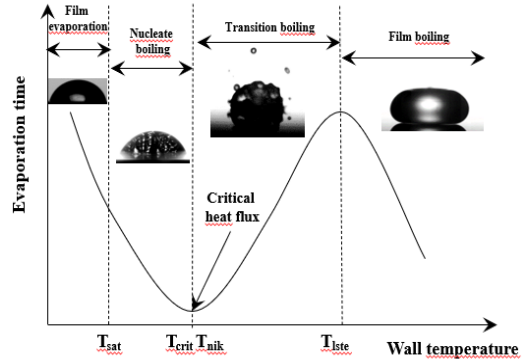


Figure 1: Droplet evaporation time as a function of wall temperature. Four heat transfer regimes can be distinguished in the case of a sessile droplet at rest on a solid surface.

ture strongly depends on the energy of the impinging droplets over the surface energy as determined by the Weber number (Eqn.1)

$$W_e = \frac{\rho v^2 D_0}{\sigma} \quad \text{Webernumber} \quad (1)$$

In this equation, ρ is the liquid density, v the impacting velocity, D_0 the drop diameter and σ the surface tension. When the Weber number is low, surface tension is predominant, causing the droplet to recoil. Depending on the temperature, the droplet may either rebound or remain attached to the surface after impact. Droplets with intermediate Weber numbers recoil and bounce, although they may eventually atomize—split into smaller droplets. When a droplet has a high Weber number, its kinetic energy is so great that surface tension cannot stop it from splashing during the spreading stage, resulting in the formation of tiny droplets[5].

A spray can be produced by propelling a high-pressure liquid or using air-assisted atomization through a small orifice, known as a nozzle. In order to study the heat transfer, it is easier to study a single water droplet impact on hot surfaces rather than a spray. Upon impact on a hot, dry surface or an existing liquid film, a spray droplet can exhibit a range of behaviours, including rebound, deposition, splash, evaporation, nucleate boiling, foaming, transition boiling, and film boiling. These behaviours result from the interplay of droplet parameters and liquid-wall interactions. Notably, changes in surface characteristics can significantly influence and modify these behaviors[10, 11].

Spray cooling relies on mechanisms such as surface evaporation, forced convection from droplet impingement, increased nucleation sites, and secondary nucleation on droplets. It operates on the principle of boiling, where efficient heat transfer occurs through liquid vaporization at temperatures exceeding saturation vapour pressure, allowing substantial heat extraction at modest temperature differences. Understanding boiling processes provides valuable insights into various boiling regimes[12]. Enhancing spray cooling performance involves selecting and modifying the working fluid, optimizing spray parameters, and implementing surface engineering. Surface engineering, in particular, significantly alters surface chemical compositions, structures, or geometries, influencing fluid flow and heat transfer processes[11].

Surface modification enhances the heat transfer efficiency of spray cooling by augmenting turbulence, surface area, and wettability. Wettability and liquid behaviour on surfaces are crucial to many applications, including biological, medical, thermal management, microfluidics, and agricultural technologies. The interactions between liquid films or droplets and surfaces depend on the solid surface’s physicochemical properties, the liquid’s nature, and the surrounding environment[13, 14, 15, 16, 17].

1.1 Wetting of Water on Surfaces

Thomas Young pioneered wetting science in 1805 by defining surface wettability through the concept of a liquid’s contact angle[18]. A surface’s affinity for water is defined by the apparent contact angle θ° . For $\theta^\circ < 90^\circ$, the surface is defined as hydrophilic and for $\theta^\circ > 90^\circ$, the surface is defined as hydrophobic. The contact angle value on a solid surface is determined by the interfacial interactions or the various binary surface tensions of solid-gas (γ_{sg}), liquid-gas (γ_{lg}), and solid-liquid (γ_{sl}), as well as the force balance established at the triple phase contact line (TPCL) and is defined by the Young-Dupr’e equation(equation 2)[19].

$$\cos\theta_0 = \frac{\gamma_{sg} - \gamma_{sl}}{\gamma_{lg}} \quad \text{Young's Equation} \quad (2)$$

The wettability of solid surfaces, whether metal or non-metal, can be categorized as hydrophobic, hydrophilic, superhydrophobic, or superhydrophilic based on Eq. (2). The Young-Dupr’e equation applies to perfect, smooth, and chemically homogeneous

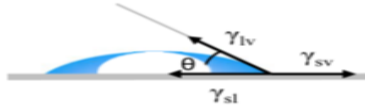


Figure 2: Triple Phase Contact Line

surfaces in thermodynamic equilibrium or immediately after droplet deposition. Wenzel connected a solid surface’s macroscopic roughness to contact angle, showing how roughness can enhance hydrophobicity. Cassie and Baxter expanded this to rough and porous surfaces, introducing the composite wetting model, which describes air trapping between a solid and water[20, 21, 22]. Techniques such as roughening, coating, and nanocoating increase the heat transfer area density. These surface modifications affect the wetting properties and ultimately impact the efficiency of spray cooling[23].

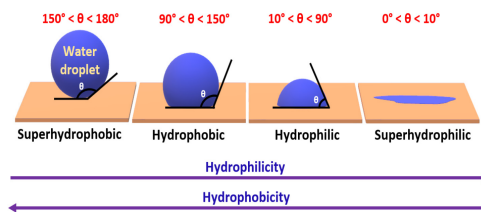


Figure 3: Diagram showing various surface wettability through contact angle measurement[24]

The wettability of surfaces is significantly influenced by atmospheric volatile organic compounds (VOCs), which are present in ambient air due to natural and industrial processes like biofuel combustion. VOCs can adsorb onto solid surfaces, with their accumulation affected by the substrate’s material and structure. The mechanisms governing surface wettability in relation to VOCs are not fully understood[18, 25]. Surfaces initially exhibit hydrophilic behavior, with water droplets spreading and forming contact angles below 40° after processes like polishing or cleaning with acids or bases. However, exposure to ambient air causes these surfaces to transition from hydrophilic to hydrophobic within hours to days, attributed to interactions with atmospheric VOCs[26, 27].

Löblein, S. M., et. al., investigated how storage circumstances had a significant impact on how mechanically polished copper surfaces developed their wetting behaviour. Following sample preparation, they saw a shift from hydrophilic to hydrophobic, which was impacted by the wrapping paper, which acted as a donor for hydrocarbons that had previously most

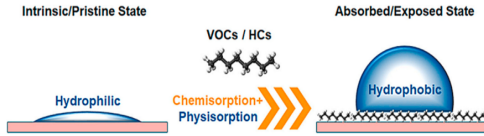


Figure 4: Schematic representation of the hydrophilic to hydrophobic wettability transition.[25]

likely been absorbed by the material from interaction with environments high in accidental carbon[28]. Utilising oxygen plasma treatment, Strohmeier effectively eliminated carbon and volatile organic compounds (VOCs) from aluminium foil, leaving behind a comparatively clean surface that showed more wetting than the uncleaned one. As demonstrated by XPS, following oxygen plasma cleaning, the wetting behaviour gradually decreased along with the adsorption of carbon-based component adsorption[29]. Copper, stainless steel (SUS), and aluminium were used in an investigation by Kim et al., following atmospheric plasma jet treatment, a noticeable reduction in the contact angle and the carbon content as determined by XPS was observed, which is consistent with the previous studies[30].

1.2 Surface Patterning

Heat flux measures energy flow per unit area over time. Critical heat flux (CHF) denotes the maximum achievable in boiling heat transfer, marking the transition from nucleate to film boiling. Film boiling reduces efficiency due to vapor film formation near the heated surface. Creating micro/nanopillars, holes, and hierarchical patterns improves heat transfer coefficient and CHF compared to smooth surfaces, particularly beneficial for demanding applications like electronics[5, 6]. Surface patterning enhances heat transfer performance by increasing surface area. Reliable techniques for surface patterning exist, but more flexible and cost-effective technologies are needed, especially for metallic surfaces. Engineered surfaces offer numerous nucleation sites and longer three-phase contact lines, optimizing latent heat utilization of the working fluid. Enhancement mechanisms depend on the length scale of surface structures, with various structures under exploration[5, 31].

Pais et al.[32] and Sehmbe et al.[33] investigated the impact of surface roughness and contact angle using a water atomized nozzle, with flow rates reaching up to $1.4\text{ml}/\text{cm}^2 \text{ s}$ for water and $400\text{ml}/\text{cm}^2 \text{ s}$ for air. Their findings revealed a decrease in heat flux with increasing surface roughness for gas atomizing nozzles. In contrast, liquid atomizing nozzles

exhibited an increase in heat flux with rising surface roughness. Additionally, they observed an enhancement in the heat transfer coefficient with decreasing surface roughness and increasing contact angle. The researchers achieved heat fluxes up to $1250\text{W}/\text{cm}^2$ at an 11°C surface superheat on an ultrasmooth ($R_a = 0.3\mu\text{m}$) copper surface. Kim et al. delved into the spray cooling dynamics of both plain and microporous coated surfaces, utilizing water at flow rates up to $0.03\text{ml}/\text{cm}^2 \text{ s}$. The microporous layer, with a maximum thickness of $500\mu\text{m}$, was created using a mixture of methyl-ethyl-ketone (MEK), epoxy, and aluminium powder. The results revealed a significant enhancement in the heat transfer coefficient, reaching up to 400% compared to the plain surface, attributed to the incorporation of microporous surfaces. Additionally, the critical heat flux (CHF) saw a 50% increase relative to the uncoated surface. However, the highest achieved heat flux was capped at $3.2\text{W}/\text{cm}^2$ at a 65°C surface superheat, a limitation attributed to the very low flow rates employed in the study[34].

Several plasma techniques, such as ion bombardment etching, carburizing, nitriding, and electrolytic oxidation, are useful for improving surface heat transfer characteristics. The primary goal of this thesis is to characterise the behaviour of water droplets evaporating on polished austenitic stainless steel AISI 316L surfaces changed by plasma treatments and alumina covered with Plasma Electrolytic Oxidation (PEO). PEO coatings generally have two layers: a dense inner layer and a porous outer layer. Oxidation time, electrical parameters, electrolyte composition and temperature, substrate type, and particle additions are some of the elements that affect the microstructure, composition, and functionality of PEO coatings[5, 6].

2 Experimental Methods

Alumina samples were surface-treated via plasma electrolytic oxidation. Three (3) samples **A**, **B** and **C** with sizes $4\times 1\text{cm}$ were immersed in alkaline electrolyte for a duration of 5, 20 and 40 minutes with alterations in parameters for each case. The PEO processing parameters altered include the voltage, current, frequency, duty cycle, particle additives, coating time, and operational temperature. The variation in coating time and processing parameters was to produce materials with different structures to observe their effect on the enhancement of heat transfer. A ($4\times 1\text{cm}$) non-polished Aluminium(**NP**) sample was also characterized. Another ($4\times 1\text{cm}$) aluminium sam-

ple (**P**) was mechanically polished until mirror-like using SiC emery paper up to 4000grit($5\mu\text{m}$). The final polishing steps involved the use of $3\mu\text{m}$ and $1\mu\text{m}$ diamond paste to achieve an arithmetical mean height Sa of 3-4nm. Cleaning was performed by immersion in an ethanol ultrasonic bath for five minutes. Samples were dried by an ambient air stream. The details of different experimental set-ups used in this study for investigating wettability, spreading and evaporation are given below:

2.1 Contact Angle Measurement

To measure the static contact angle (SCA), a Digidrop contact angle Goniometer at room temperature($22\text{-}23^\circ\text{C}$). The measurement process involves the usage of a flattened stage as a sample holder so that the droplet does not move during deposition. A droplet of distilled water(conductivity- $55\mu\Omega\text{m}^{-1}$) and (volume= $1.14\mu\text{l}$ and $d=4\text{cm}$) is deposited onto the sample with minimal influence of external forces. The droplet is illuminated from behind, and an image is recorded by the camera. The image is analysed using software, and a contact angle measurement is determined. SCA results are portrayed as the mean of multiple measurements with error bars indicating the standard deviation. Before measurements, the samples were cleaned using ethanol and distilled water and dried in ambient air.

2.2 Spreading Dynamics

The sample is maintained on a stationary platform while the droplet spreading dynamics are investigated. The droplet is carefully applied to the sample using a needle ($d=200\mu\text{m}$), with a syringe pump regulating the droplet volume. The samples are heated to varying degrees of temperature and the droplet behaviours are observed. The Spreading dynamics are captured by high-speed photography (Fastcam-Photron® SA-3, resolution 1024×1024 at 2000 frames per second). To determine the behaviour at different Weber numbers, the drop height is varied at 5, 10 & 20cm.

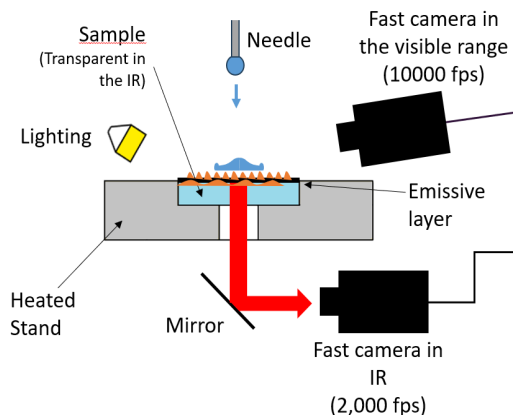


Figure 5: Experimental set-up for spreading dynamics measurement and observation.

3 Result

The PEO-coated samples were observed under a Scanning Electron Microscope(SEM) to view their surface structures, noticing observable differences (Figs 6-8). After their observation, the static contact angles were measured and the time variation effect was recorded as depicted in Fig.9. The spreading dynamics were then investigated at 3 different heights (5,10 & 20cm), representing 3 different Weber numbers of 26.95, 53.90 & 107.80. The behaviour of the drop at different temperatures (80, 100, 125, 150, 175 & 200°C) was also observed. Figs.10-16 show the progression of the drop from the initial contact with the surface to the final drop evaporation/absorption. The behaviours of the drop are captured at different temperatures($80, 100, 125, 150$ & 175°C), and three samples are represented: **A**, **NP** & **P** This duration from the initial drop to the final evaporation indicates the drop's lifetime. Fig. 16 shows the lifetime of the drop as measured against the varying temperatures for all samples, including the polished and non-polished pure Aluminium samples. At 80°C , Samples **A**, **B** & **C** were measured to observe the effect of Weber variation on the drop lifetime as shown in Fig.18. For each temperature, multiple experiments are performed with the error being 3ms. The static contact angles were then re-measured to observe the changes after they had been subjected to the projection of droplets at high temperatures(Fig.19).

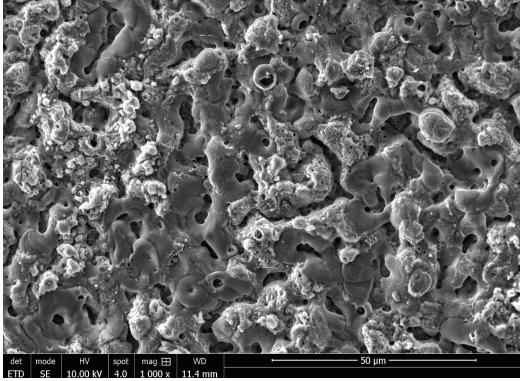


Figure 6: SEM Image of the surface for **A**

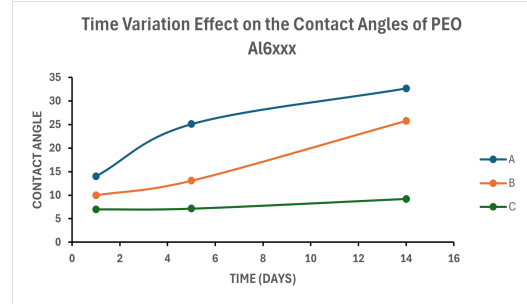


Figure 9: Initial CA Variation with Time for PEO Al6xxx samples.

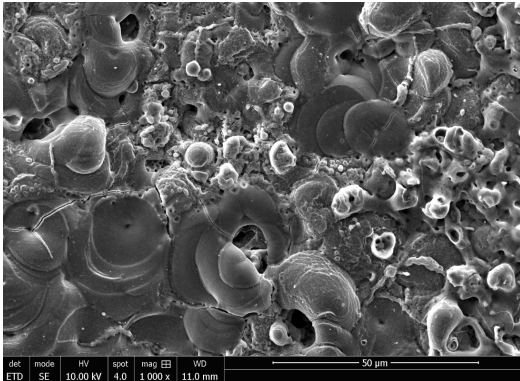


Figure 7: SEM Image of the surface for **B**

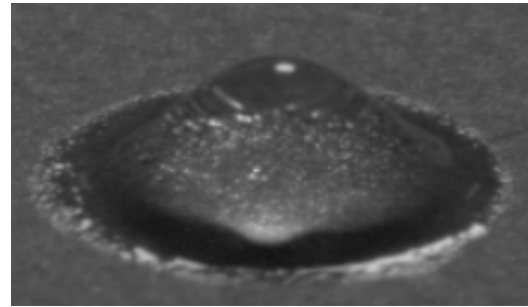


Figure 10: Drop Deposition @ 0.026s (Sample **A**: $h = 5\text{cm}$; $T = 80^\circ\text{C}$)

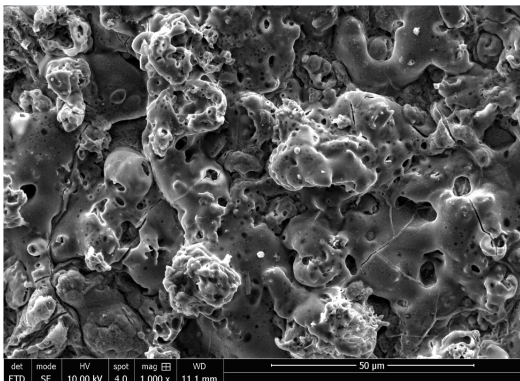


Figure 8: SEM Image of the surface for **C**

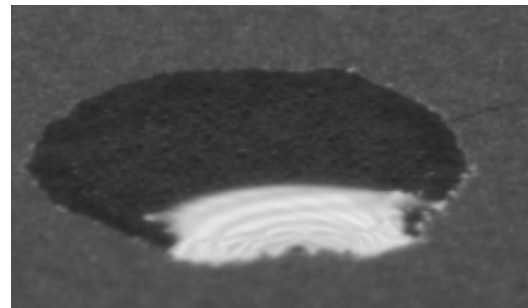


Figure 11: Drop Spreading @ 23.24s (Sample **A**: $h = 5\text{cm}$; $T = 80^\circ\text{C}$)

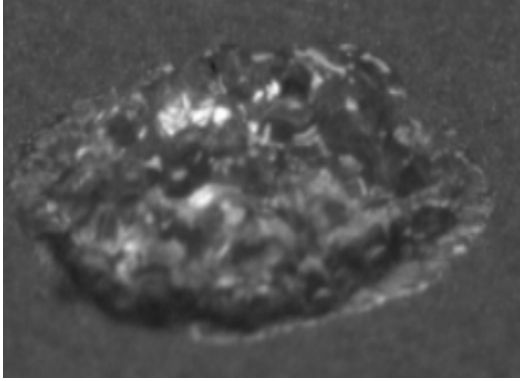


Figure 12: Drop Ebullition @ 0.33s (Sample **A**: $h = 5\text{cm}$; $T = 100^\circ\text{C}$)

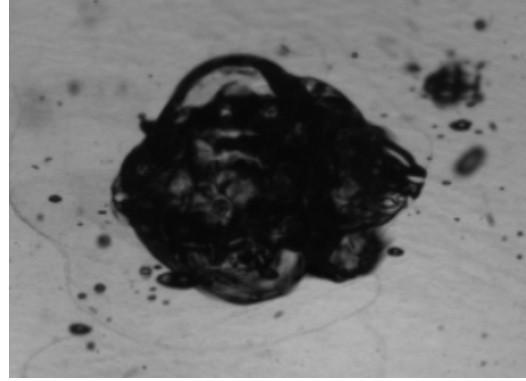


Figure 15: Thermal Atomization @ 0.186s (Sample **NP**: $h = 20\text{cm}$; $T = 125^\circ\text{C}$)

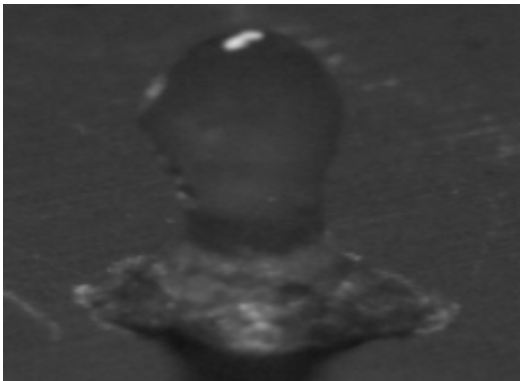


Figure 13: Drop Dancing @ 0.0197s (Sample **A**: $h = 5\text{cm}$; $T = 150^\circ\text{C}$)

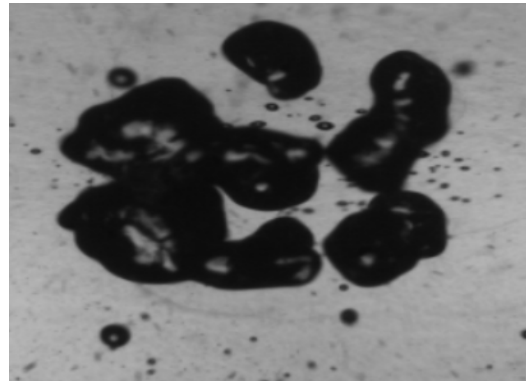


Figure 16: Thermal Atomization and droplet breakup @ 0.106s (Sample **P**: $h = 20\text{cm}$; $T = 175^\circ\text{C}$)

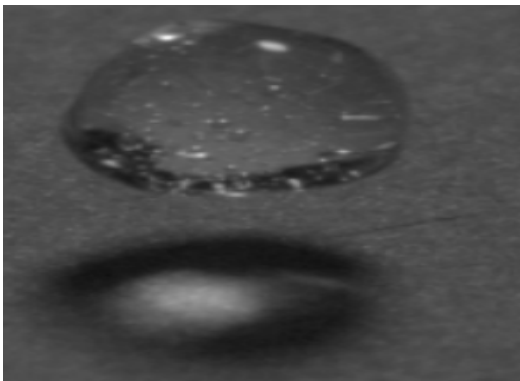


Figure 14: Drop Rebound @ 0.709s (Sample **A**: $h = 5\text{cm}$; $T = 175^\circ\text{C}$)

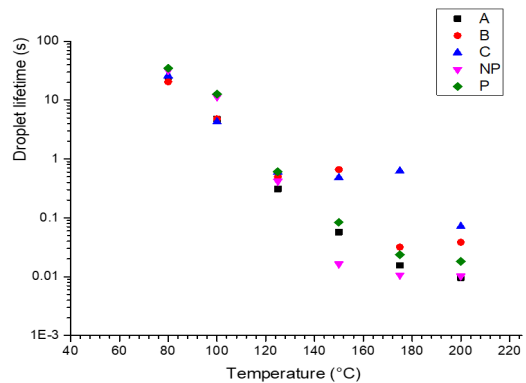


Figure 17: Influence of Temperature on Drop Lifetime for samples A, B, C and non-treated aluminium samples (NP: non-polished and P: polished)

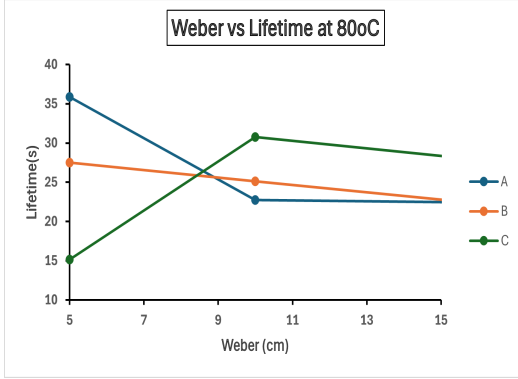


Figure 18: Weber Number impact on lifetime

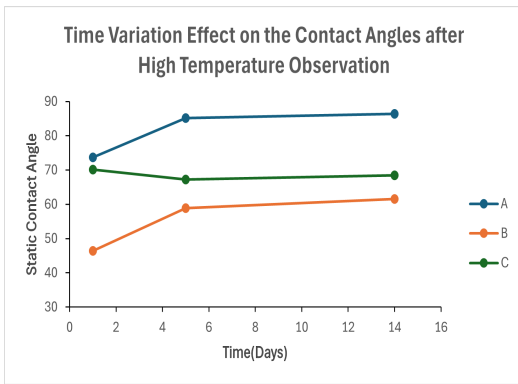


Figure 19: Change in static CA after High-Temperature Observation

4 Discussion

The PEO-coated samples displayed micro-holes that changed in size and shape due to the application of various duty cycles and frequencies. Figs. 6-8 demonstrate the differences in the porous nature of the samples. Sample C is shown to have greater porosity than A and B. This implies that it can promote more liquid spreading due to capillary action, leading to a lower apparent contact angle as seen in Fig. 9. Conversely, the lower porosities of A & B suggest the lower penetration of liquid, leading to higher contact angles and reduced wetting. The static contact angle follows a linear time evolution. The increase in contact angle can be attributed to the adsorption of volatile organic substances on the surface of the samples.

Different impact regimes (Figs. 10-16) are produced by the drop impact on a hot substrate due to the interaction of both thermodynamic and hydrodynamic variables, in contrast to isothermal impacts. Single-phase cooling drop deposits occur at surface temperatures below the saturation temperature (T_{sat}). Nu-

cleate boiling takes place above T_{sat} , causing bubbles to develop in the liquid sheet. Partial drop rebound and the "drop dancing" regime, characterised by bubble merging and transitional boiling, happen as the temperature climbs even higher. Thermal atomisation or complete drop rebound occurs at even greater temperatures, particularly at high-impact velocities where viscous forces predominate [35]. Fig. 16 shows droplet breakup accompanying thermal atomization at 175°C on the polished aluminium surface. Due to the hydrophilic nature of **P** and the absence of surface roughness, droplet breakup is encouraged and the Leidenfrost effect is intensified. In addition, the droplet breaks apart due to vapour-induced forces, a rapid rate of heat transfer, and a violent interaction (excessive boiling) between the droplet and the hot surface.

The lifetime of a drop refers to the duration a liquid droplet remains on a surface before it either evaporates completely or is absorbed. It influences heat transfer efficiency, cooling rates, and surface interaction dynamics. From Fig. 17, the impact of temperature on drop lifetime can be observed. For all samples, at lower temperatures, the effect is negligible, but as the temperature increases, the effect becomes more evident. At 100°C, the PEO-coated samples show a shorter drop lifetime than the pure Aluminium samples, whereas, at higher temperatures, the **P** & **NP** show a shorter drop lifetime. Shorter drop lifetimes generally mean quicker evaporation, which is desirable for rapid heat transfer and cooling. This implies that samples **NP** & **P** can be utilized for high heat flux applications in technologies requiring rapid cooling. Longer lifetimes suggest slower evaporation, which is great for sustained cooling applications, as it might result in more uniform cooling. Also, longer droplet lifetimes are frequently associated with improved surface wettability and contact, which can raise heat transfer efficiency overall by facilitating processes like nucleate boiling. It can also reduce thermal stresses in materials by contributing to more gradual cooling. This implies that **A**, **B** & **C** can be utilized in industrial processes that require slow and controlled cooling.

For samples **A** & **B**, at a particular temperature (80°C), Weber number and drop lifetime follow an inverse relationship. As depicted in Fig. 18, an increase in Weber number leads to a decrease in lifetime. At low Weber numbers, surface tension forces dominate over inertial forces resulting in the droplet spreading gently upon impact and staying on the surface for a longer time since it is not subject to significant disruptive forces that would cause it to spread, splash, or break apart. A droplet's lifetime is shortened at

high Weber numbers due to the dominance of inertial forces over surface tension, which causes significant droplet deformation, spreading, splashing, or even fragmentation. These events decrease the amount of time the liquid is in contact with the surface as the droplet breaks up into smaller ones, spreads thinly over the surface, or completely rebounds off it. For sample C, which is more hydrophilic, an anomaly is observed. A lower Weber number frequently leads to a shorter droplet lifetime on a highly porous and hydrophilic surface because the droplet is rapidly absorbed by the surface. In contrast, the droplet may spread and interact with the surface for a longer period before being absorbed in a higher Weber number due to the increased kinetic energy. This could result in an extended lifetime. The observed variance in droplet lifetime across different Weber numbers is explained by the interaction of impact energy, surface properties, and fluid dynamics.

Fig. 19 shows the changes in SCA of **A, B & C** after the projection of drops at high temperatures. The changes were observed for 14 days to notice any differences that might have occurred before and after the high-temperature droplet projection. A & B follow a linear progression, as SCA increases with time. Comparing Fig. 9 with Fig. 19, a shift in SCA is observed, as the samples transition from higher hydrophilicity to lower hydrophilicity. This transition could also be the effect of the adsorption of VOCs present in the atmosphere. As with Fig. 18, C shows an anomaly in the SCA with time. The intricate interactions between liquid characteristics, surface chemistry, and external influences are reflected in the dynamic behaviour of the contact angle over time. An initial high contact angle may result from early conditions like pollution from VOCs. The contact angle may be lowered by spreading or absorption as the liquid interacts with the surface. Eventually, the contact angle may rise once more as a result of evaporation or surface recovery activities.

5 Conclusions

In this work, the sessile and projected droplet approaches were used to examine the heat transfer characteristics of PEO-coated alumina, polished, and non-polished aluminium samples. At room temperature, the initial and final contact angles of the samples were displayed as functions of time. The PEO-coated samples with lower contact angles were shown to be generally hydrophilic to varying degrees, while the pure aluminium samples generally tended towards hydrophobicity. The behaviour of the projected drop

at high temperatures was observed and the drop lifetime was presented as a function of the temperatures. The effect of the Weber number was also studied. The results indicate that PEO-coated samples can be utilized in low heat-flux applications requiring slow, sustained and gradual cooling as they have longer lifetimes, while the pure aluminium samples can be utilized for high heat-flux applications requiring rapid cooling. In spray cooling, both short and long droplet lives have advantages; the best droplet lifetime will rely on the particular cooling needs of the application. Reaching the ideal droplet lifetime frequently necessitates striking a balance. By adjusting the nozzle design, spray angle, droplet size, and spray pressure, this balance can be reached. Changes to surface characteristics like wettability, roughness, and material composition can also have an impact on droplet lifetime and behaviour. To achieve efficient and effective spray cooling, it is essential to balance these elements by careful design and optimisation of the spray parameters, surface features, and fluid properties.

Acknowledgements

The author would like to acknowledge Prof. Thierry Czerwiec for his supervision and guidance in the course of this work. The author would also like to thank Profs. Guillaume Castanet, Gregory Marcos, Ophélie Caballina, Julien Martin, Thomas Potafeux (PhD.) and Erwan Etienne for their assistance in the experimental process and analysis of this study. A special thanks to Moussa Mancer and Leo Pereire for their support in this work. The author graciously appreciates her family and friends for their constant support and care during the research and production of this study. And finally, the author would like to acknowledge The Almighty God, the author of wisdom and strength. This study was carried out at the Institut Jean Lamour (IJL) in collaboration with LEMTA under the University of Lorraine, France.

References

- [1] D J Lee. Bubble Departure Radius Under Microgravity. *Chemical Engineering Communications*, 117(1):175–189, 9 1992.
- [2] Huseyin Bostanci, Daniel P Rini, John P Kizito, Virendra Singh, Sudipta Seal, and Louis C Chow. High heat flux spray cooling with ammonia: Investigation of enhanced surfaces for HTC. *International Journal of Heat and Mass Transfer*, 75:718–725, 2014.

- [3] Wen-Long Cheng, Wei-Wei Zhang, Hua Chen, and Lei Hu. Spray cooling and flash evaporation cooling: The current development and application. *Renewable and Sustainable Energy Reviews*, 55:614–628, 2016.
- [4] Cheng-Chieh Hsieh and Shi-Chune Yao. Evaporative heat transfer characteristics of a water spray on micro-structured silicon surfaces. *International Journal of Heat and Mass Transfer*, 49(5):962–974, 2006.
- [5] T Czerwiec, Svetlana Tsareva, A Andrieux, G Bortolini, P Bolzan, Guillaume Castanet, Grdeck Michel, and Grégory Marcos. Thermal management of metallic surfaces: evaporation of sessile water droplets on polished and patterned stainless steel. *IOP Conference Series: Materials Science and Engineering*, 258:012003, 10 2017.
- [6] Zhibin Yan, Rui Zhao, Fei Duan, Teck Wong, Kok Toh, Kok Choo, Poh Chan, and Yong Chua. Spray Cooling. 9 2011.
- [7] J D Benthier, J D Pelaez-Restrepo, C Stanley, and G Rosengarten. Heat transfer during multiple droplet impingement and spray cooling: Review and prospects for enhanced surfaces. *International Journal of Heat and Mass Transfer*, 178:121587, 2021.
- [8] Jiameng Tian, Bin Chen, and Dong Li. Light transmittance dynamics and spectral absorption characteristics during auxiliary cryogen spray cooling in laser dermatology. *Lasers in Medical Science*, 37(3):2079–2086, 2022.
- [9] Tianshi Zhang, Ziming Mo, Xiaoyu Xu, Xiaoyan Liu, Haopeng Chen, Zhiwu Han, Yuying Yan, and Yingai Jin. Advanced Study of Spray Cooling: From Theories to Applications. *Energies*, 15(23), 2022.
- [10] Sameer Khandekar, Ankush Kumar Jaiswal, and Gopinath Sahu. Chapter Four - Spray cooling: From droplet dynamics to system level perspectives. volume 54 of *Advances in Heat Transfer*, pages 135–177. Elsevier, 2022.
- [11] Ruina Xu, Gaoyuan Wang, and Peixue Jiang. Spray Cooling on Enhanced Surfaces: A Review of the Progress and Mechanisms. *Journal of Electronic Packaging*, 144(1), 8 2021.
- [12] M Jena, P C Mishra, and S S Sahoo. Spray Impingement Cooling of Metal Surfaces: a Review on Progressing Mechanisms. *Thermal Engineering*, 70(8):573–594, 2023.
- [13] Zhen Zhang, Jia Li, and Pei-Xue Jiang. Experimental investigation of spray cooling on flat and enhanced surfaces. *Applied Thermal Engineering*, 51(1):102–111, 2013.
- [14] Tatiana Gambaryan-Roisman and Victor Starov. Editorial overview: Recent progress in studies of complex wetting and spreading phenomena. *Current Opinion in Colloid & Interface Science*, 55:101486, 2021.
- [15] Yifan Si, Cunlong Yu, Zhichao Dong, and Lei Jiang. Wetting and spreading: Fundamental theories to cutting-edge applications. *Current Opinion in Colloid & Interface Science*, 36:10–19, 2018.
- [16] Yichuan Zhang, Mingming Guo, David Seveno, and Joël De Coninck. Dynamic wetting of various liquids: Theoretical models, experiments, simulations and applications. *Advances in Colloid and Interface Science*, 313:102861, 2023.
- [17] Zhenying Wang, Daniel Orejon, Yasuyuki Takata, and Khellil Sefiane. Wetting and evaporation of multicomponent droplets. *Physics Reports*, 960:1–37, 2022.
- [18] Xiongjiang Yu, Carlos Alberto Dorao, and Maria Fernandino. Droplet evaporation during dropwise condensation due to deposited volatile organic compounds. *AIP Advances*, 11(8):085202, 8 2021.
- [19] Malcolm E Schrader. Young-Dupre Revisited. *Langmuir*, 11(9):3585–3589, 9 1995.
- [20] By Thomas Young and M D For Sec. HI, An Essay on the Cohesion of Fluids. Technical report.
- [21] Robert N Wenzel. RESISTANCE OF SOLID SURFACES TO WETTING BY WATER. *Industrial & Engineering Chemistry*, 28(8):988–994, 8 1936.
- [22] A B D Cassie and S Baxter. Wettability of porous surfaces. *Transactions of the Faraday Society*, 40(0):546–551, 1944.
- [23] Saeed Thakur, Santosh Kadapure, Prasad Hegde, and Umesh Deshannavar. A Review of Parameters and Mechanisms in Spray Cooling. *Metalurgical and Materials Engineering*, 29(3):36–64, 10 2023.

- [24] Subodh Barthwal, Surbhi Uniyal, and Sumit Barthwal. Nature-Inspired Superhydrophobic Coating Materials: Drawing Inspiration from Nature for Enhanced Functionality. *Micromachines*, 15(3), 2024.
- [25] Daniel Orejon, Junho Oh, Daniel J Preston, Xiao Yan, Soumyadip Sett, Yasuyuki Takata, Nenad Miljkovic, and Khellil Sefiane. Ambient-mediated wetting on smooth surfaces. *Advances in Colloid and Interface Science*, 324:103075, 2024.
- [26] Junho Oh, Daniel Orejon, Wooyoung Park, Hyeongyun Cha, Soumyadip Sett, Yukihiko Yokoyama, Vincent Thoreton, Yasuyuki Takata, and Nenad Miljkovic. The apparent surface free energy of rare earth oxides is governed by hydrocarbon adsorption. *iScience*, 25(1):103691, 2022.
- [27] Satoshi Takeda, Makoto Fukawa, Yasuo Hayashi, and Kiyoshi Matsumoto. Surface OH group governing adsorption properties of metal oxide films. *Thin Solid Films*, 339(1):220–224, 1999.
- [28] Sarah Marie Löfflein, Rolf Merz, Daniel Wyn Müller, Michael Kopnarski, and Frank Mücklich. An in-depth evaluation of sample and measurement induced influences on static contact angle measurements. *Scientific Reports*, 12(1), 12 2022.
- [29] B R Strohmeier. The Effects of O₂ Plasma Treatments On The Surface Composition and Wettability of Cold-Rolled Aluminum Foil. *Journal of Vacuum Science and Technology A: Vacuum, Surfaces and Films*, 7(6):3238–3245, 1989.
- [30] M C Kim, S H Yang, J.-H. Boo, and J G Han. Surface treatment of metals using an atmospheric pressure plasma jet and their surface characteristics. *Surface and Coatings Technology*, 174-175:839–844, 2003.
- [31] Rui-Na Xu, Lei Cao, Gao-Yuan Wang, Jian-Nan Chen, and Pei-Xue Jiang. Experimental investigation of closed loop spray cooling with micro- and hybrid micro-/nano-engineered surfaces. *Applied Thermal Engineering*, 180:115697, 2020.
- [32] M R Pais, L C Chow, and E T Mahefkey. Surface Roughness and Its Effects on the Heat Transfer Mechanism in Spray Cooling. *Journal of Heat Transfer*, 114(1):211–219, 2 1992.
- [33] M. S. Sehmbe, M. R. Pais, and L. C. Chow. Effect of surface material properties and surface characteristics in evaporative spray cooling. *Journal of Thermophysics and Heat Transfer*, 6(3):505–512, 9 1992.
- [34] J H Kim, S M You, and Stephen U S Choi. Evaporative spray cooling of plain and microporous coated surfaces. *International Journal of Heat and Mass Transfer*, 47(14):3307–3315, 2004.
- [35] Jan Breitenbach, Ilia Roisman, and Cameron Tropea. Heat transfer in the film boiling regime: Single drop impact and spray cooling. *International Journal of Heat and Mass Transfer*, 110:34–42, 7 2017.